Task 5.4: Hydromechanical analysis of cyclic hydraulic stimulation in Pohang fractured geothermal reservoir, South Korea

GFZ Helmholtz Centre POTSDAM

DESTRESS — Demonstration of soft stimulation treatments of geothermal reservoirs

Márton Farkas[1,2] Hannes Hofmann[2] Günter Zimmermann[2] Arno Zang[1,3] Falko Bethmann[4] Peter Meier[4] Mark Cottrell[5] Neal Josephson[5]

1 Institute for Geosciences, University of Potsdam, Potsdam, Germany
2 Section 4.8 Geoenergy, German Research Centre for Geosciences, Potsdam, Germany
3 Section 2.6 Seismic Hazard and Risk Dynamics, German Research Centre for Geosciences, Potsdam, Germany
4 Geo-Energie Suisse AG, Zürich, Switzerland
5 Golder Associates (UK) Ltd, Bourne End, United Kingdom

Questions?
farkas@gfz-potsdam.de

1 Project background

An Enhanced Geothermal System (EGS) is an engineered reservoir, in which hot dry rock with intrinsic insufficient natural permeability is stimulated hydraulically.
Enhancing permeability in a safe way is challenging (Zang et al., 2013). One option to do so, is a soft stimulation treatment enhancing permeability while induced seismicity is kept below a safe threshold. This is demonstrated at Pohang EGS site, South Korea (Fig. 1, Hofmann et al., 2019).

In this study, we investigate the hydraulic stimulations conducted at Pohang site using the 3D finite-element code FracMan (Golder Associates 2019). We focus on studying coupled processes using the dataset of soft stimulation reported in Hofmann et al., 2019 in August 2017 in well PX-1 (Fig. 2). This enables characterizing the fractured crystalline reservoir.

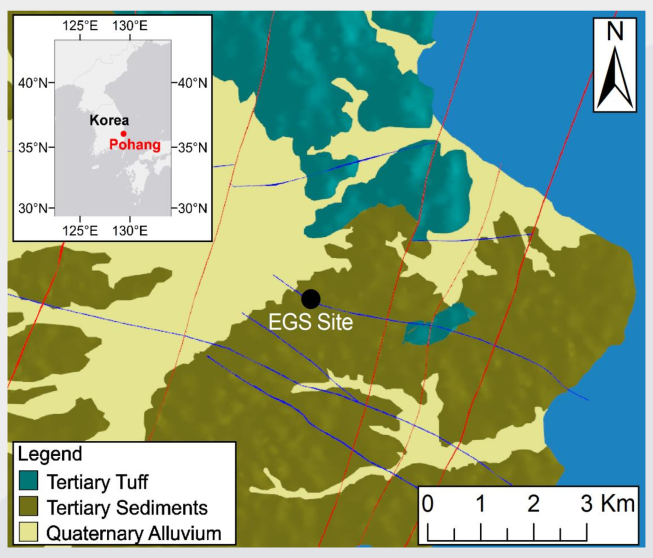

Fig. 1 Geological features at Pohang EGS Site (Hofmann et al., 2019)

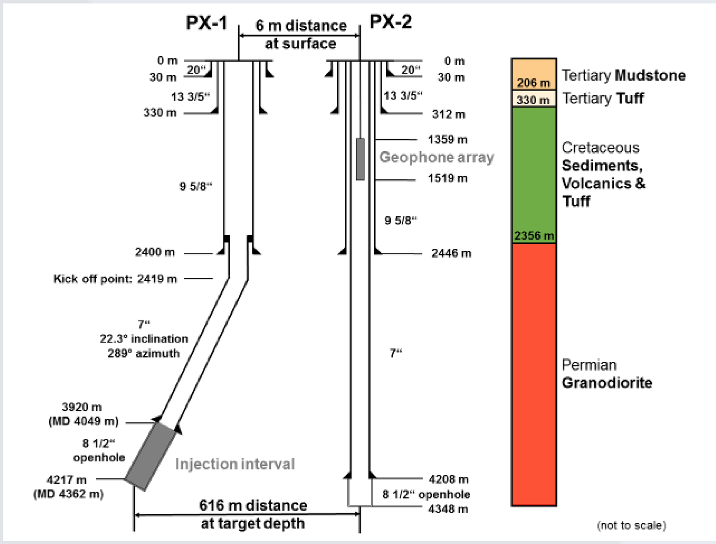

Fig. 2 Well completions including injection location and geophone chain (Hofmann et al., 2019)

2 Hydraulic Stimulations

Five stimulations were conducted in granodiorite rock to improve the hydraulic performance of the system (Fig. 3). Based on hydraulic and seismological analysis of the stimulations and earthquakes, two large fault structures are inferred, planes P1 and P2 (Fig. 4, Bethmann et al., 2019).

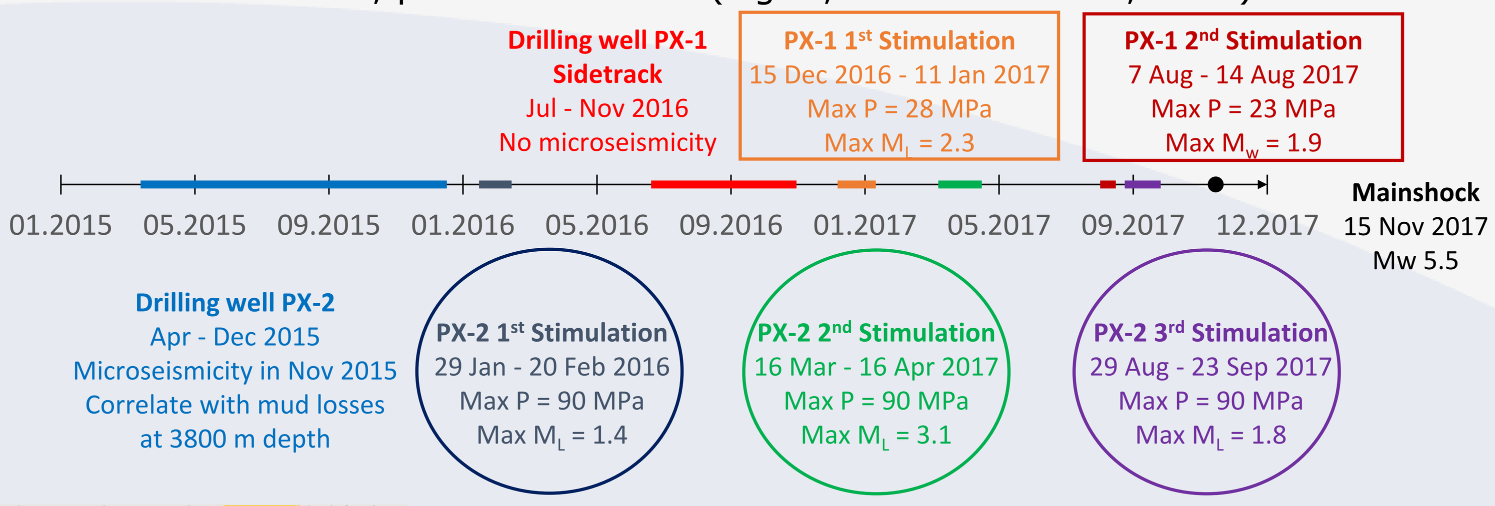

Fig. 3: Timeline of the Pohang EGS Project

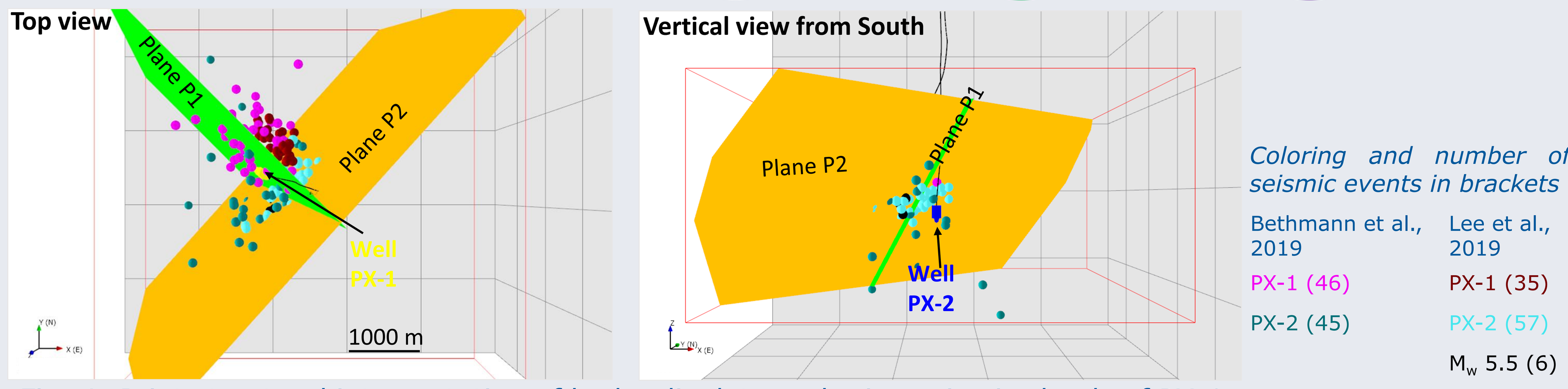

Fig. 4: Joint structural interpretation of hydraulic data and microseismic clouds of PX-1 and PX-2 hydraulic stimulations (after Bethmann et al., 2019)

3 Numerical Method and Setup

The numerical method and model of hydro-mechanical coupling for simulating fluid injection is illustrated in Fig. 5 and Fig. 6 using the equations (1)-(4).

Eq. (1) $$E_0 = \frac{JRC}{5}\left(0.2\frac{UCS}{JCS} - 0.1\right)$$

Eq. (2) $$\Delta E = \frac{\sigma_n V_m}{V_m K_n + \sigma_n}$$

Eq. (3) $$e = \frac{E^2}{JRC^{2.5}}$$

Eq. (4) $$S\frac{\partial P}{\partial t} - T\nabla^2 P = q$$

E_0 = Mechanical aperture at $\sigma_n = 0$
JRC = Joint Roughness Coefficient
UCS = Uniaxial Compressive Strength
JCS = Joint Wall Compression Strength
ΔE = Change in Mechanical Aperture
σ_n = Effective Normal Stress
V_m = Maximum Aperture Closure
K_n = Fracture Stiffness

S = Fracture Storativity
P = Fluid Pressure
T = Fracture Transmissivity
Q = Flow rate

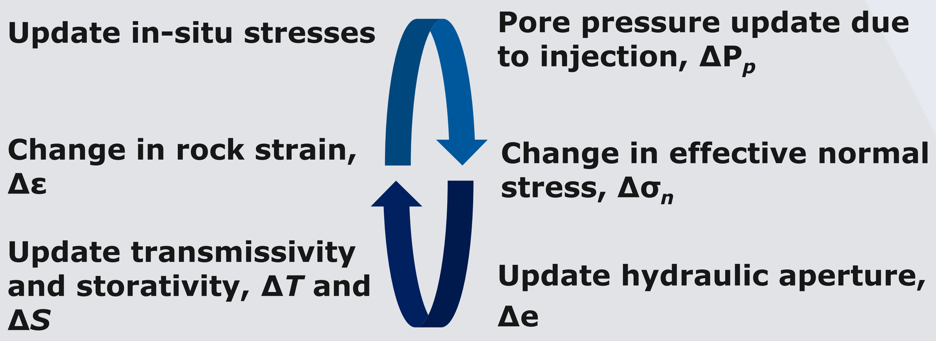

Fig. 5: Calculation cycle of hydro-mechanical coupling

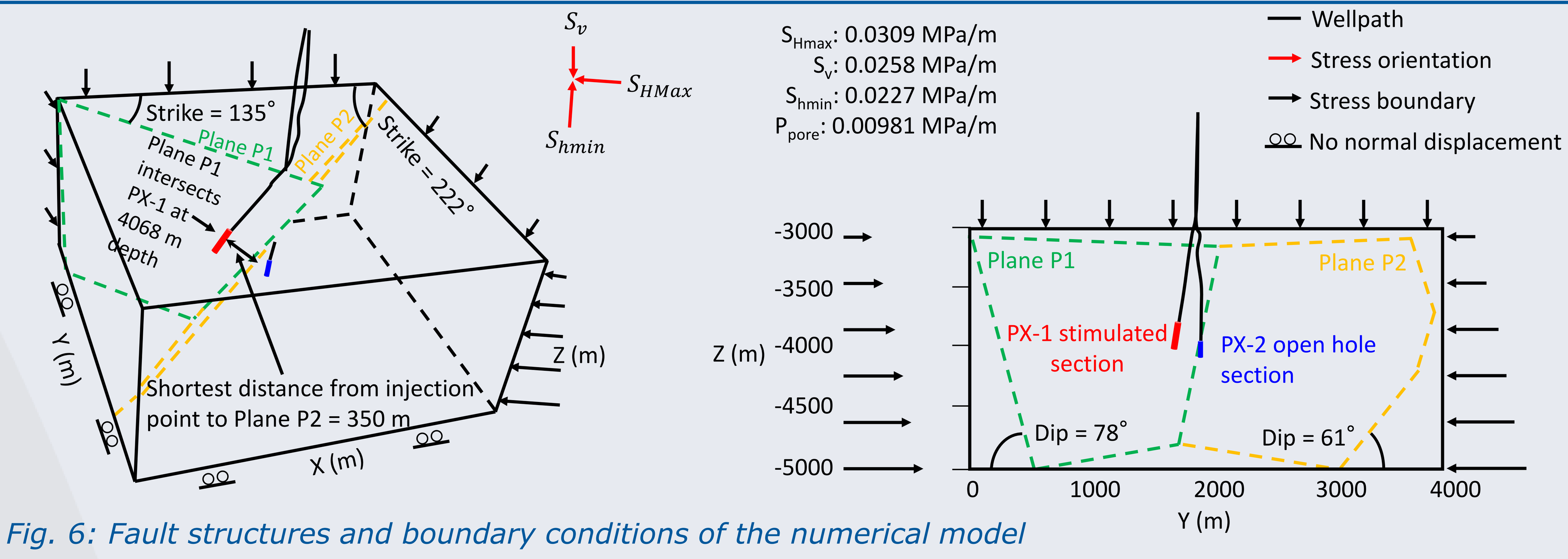

Fig. 6: Fault structures and boundary conditions of the numerical model

4 Results and Discussion

A. History matching of PX-1 2nd stimulation in August 2017

The model calibration is made by matching the simulated wellhead pressure history against field observations. The procedure requires adjusting the input parameters governing the hydro-mechanical coupling sequentially. These are referred to as split-points dividing the simulation into sequences (Fig. 7).

At the time of change in parameters, the pressure output of the last time step is taken as split-point for the subsequent phase of the simulation. These parameters remain valid for a period until the next split-point is defined.

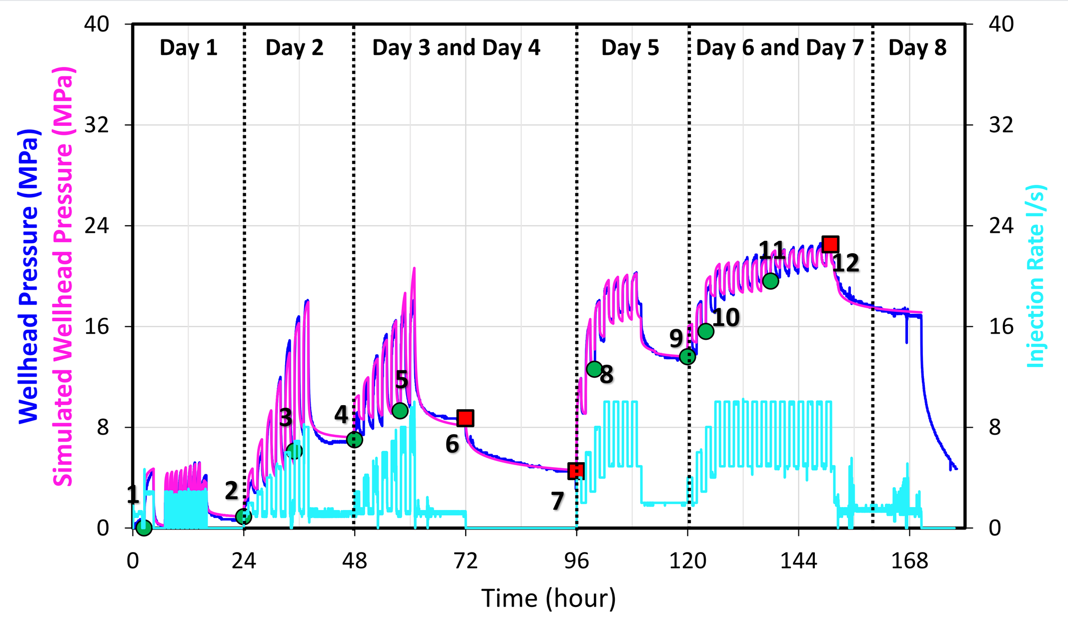

Fig. 7: Comparison of recorded and modelled wellhead pressure data for treatment in well PX-1 of August 2017. Circles represent increase in hydraulic aperture. Squares represent decrease in hydraulic aperture

The constant parameters used in the simulation are summarized in Table 1. Those that are adjusted are shown in Table 2. Based on the achieved history match, we characterize the resulting wellbore and hydro-mechanical parameters.

Table 1: Constant numerical parameters of the simulation

Parameter	Value	Parameter	Value
Well Effect		**Fault hydrogeological property**	
Well radius	0.108 m	Fault compressibility	4.5 10^{-10} 1/Pa
Fluid properties		**Geomechanical property**	
Fluid viscosity	0.3 mPa s	Normal stiffness	1300 MPa/mm
Fluid density	1000 kg/m³	Friction angle	12 deg
Matrix property		JRC	12 deg
Matrix permeability	0.1 10^{-15} m²	JCS	105 MPa
Matrix compressibility	4.5 10^{-10} 1/Pa	Maximum closure	1 mm
Numerical block radius	15 m		

Table 2: Adjusted numerical parameters of the simulation

Parameter	Day 1	Day 2		Day 3- Day 4			Day 5		Day 6 – Day 7			Day 8
Split-point ID	1	2	3	4	5	6	7	8	9	10	11	12
Well Storage (10^{-7} m³/Pa)	5	8	0.4	0.8	20	2	10	1	0.8	5	50	50
UCS (MPa)	103	105	108	108	114	105	105	113	115	117	120	115

B. Hydraulic aperture and transmissivity evolution

The change in stress-aperture relationship due to UCS adjustment results in shift of the stress-aperture relationship. The increase in UCS shifts the curve upwards, the decrease in that has opposite effect (Fig. 8).

The evolution of aperture at the borehole shows non-linear behavior and reversibility with pressure change, typical for hydraulic jacking. On the other hand, welltest analyses of hydraulic stimualtions in well PX-1 revealed hydro-shearing (Hofmann et al., 2019; Lee et al., 2019).

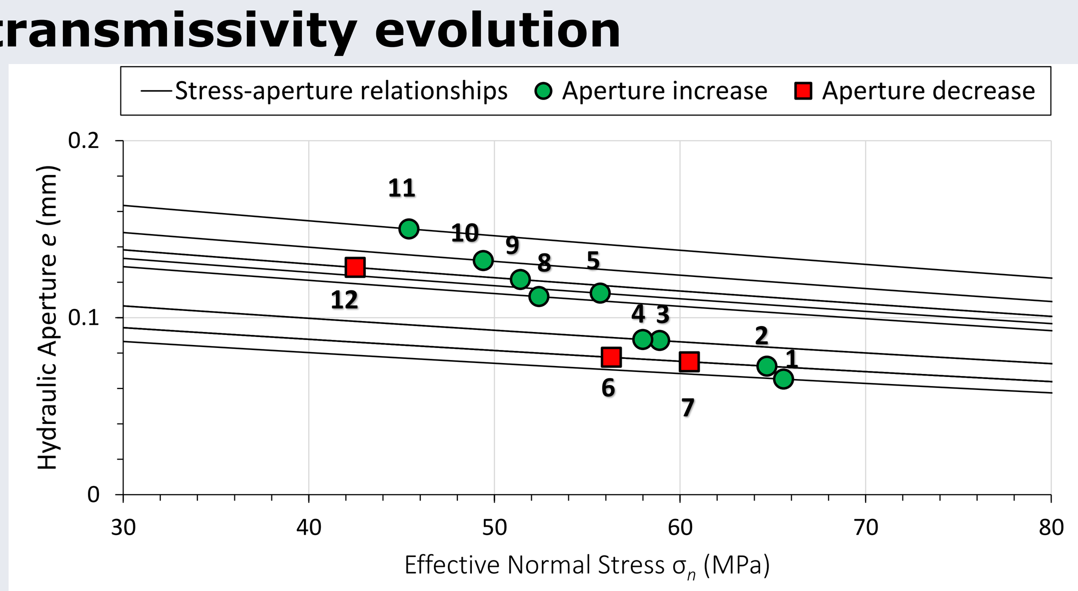

Fig. 8: Evolution of stress-aperture relationships as well as hydraulic aperture at injection point (Table 2)

Hydraulic aperture at injection point is converted to transmissivity as follows:

Eq. (5) $$T = \frac{\rho_{fluid} g e^3}{12\eta_{fluid}}$$

e = Hydraulic aperture
ρ_{fluid} = Fluid Pressure
η_{fluid} = Fluid Transmissivity

The transmissivity shows an increase in the order of one magnitude approx. from 10^{-6} to 10^{-5} m²/s (Fig. 9). This generally agrees with that reported by Hofmann et al., 2019 at different periods of the hydraulic stimulation.

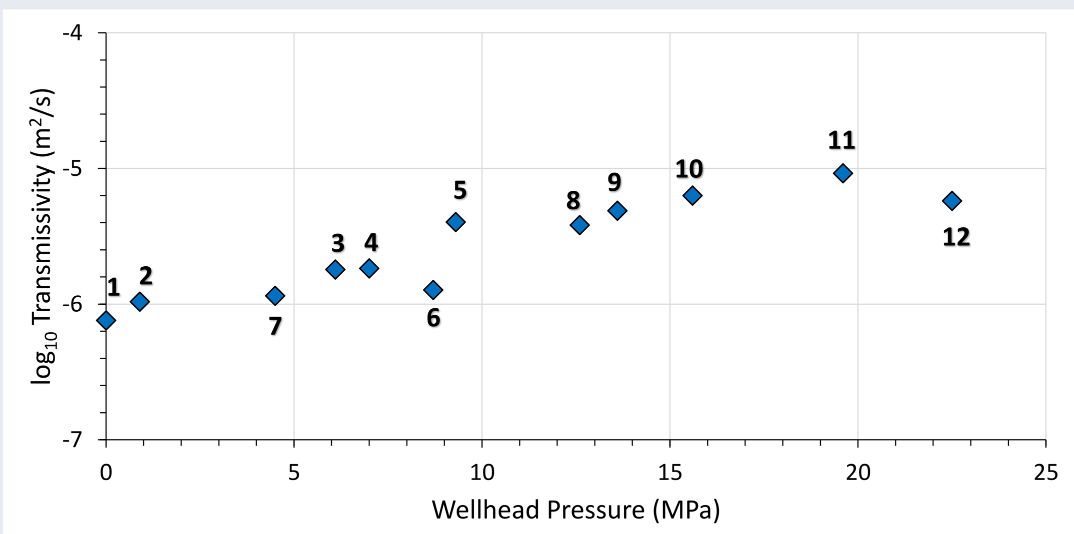

Fig. 9: Evolution of transmissivity at the injection point (Table 2)

C. Extent of pressurized area

The extent of overpressure area (Lee et al., 2019) with radius of 150 m for 0.01 MPa overpressure level implies that the hydraulic diffusion is limited relatively close to borehole area (Fig. 10).
Given that the simulated injection point is located approx. 350 m as shortest distance from plane P2, the modelling results reveal that the pore pressure, and thus, the effective stresses at fault P2 are probably not affected by PX-1 2nd stimulation.

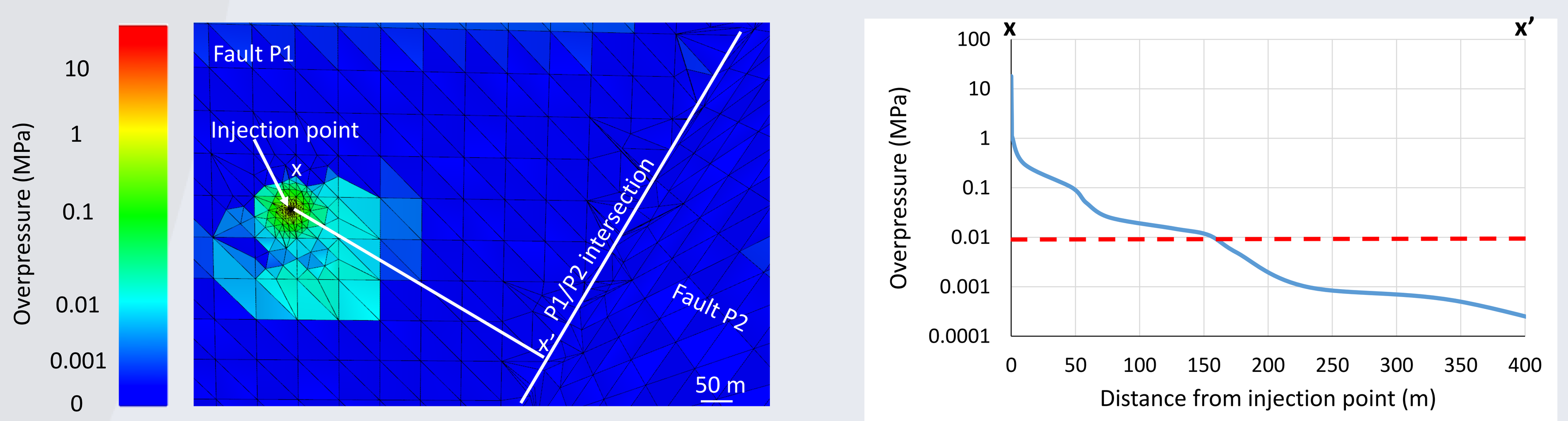

Fig. 10: The extent of pressurized subsurface area at the end of the August 2017 stimulation in well PX-1 before flowback and overpressure profile along section x-x'

5 Conclusions

- Reasonable history matching of pressure curves could only be achieved by partitioning the treatment into separate periods. This enables capturing change in hydraulic aperture and wellbore storage.
- The hydraulic aperture evolution is typical of hydraulic jacking. However, the fault is favorably oriented for hydro-shearing. This implies that the stimulation mechanism could be a combination of hydraulic jacking and shearing.
- The extent of pore pressure difference for inducing potential seismic events, is approx. 150 m in the direction of the shortest possible distance to the plane P2 based on the numerical simulations. Thus, the effective stresses at fault P2, which is located approx. 350 m are probably not affected within the model limitations.

Acknowledgements

The DESTRESS project has received funding from the European Union's Horizon 2020 research and innovation program under grant agreement No 691728. First and second author are funded by this project.

www.gfz-potsdam.de

References

- Bethmann, F., Ollinger, D., Tormann, T., 2019. Seismicity analysis with spatial or temporal relation to the deep geothermal project in Pohang during 2016/2017. Geo-Energie Suisse AG, Zürich, Switzerland.
- Golder Associates, 2019. FracMan Interactive Discrete Feature Data Analysis, Geometric Modeling and Exploration Simulation, User Documentation, v7.8
- Hofmann, H., Zimmermann, G., Farkas, M., Huenges, E., Zang, A., Leonhardt, M., Kwiatek, G., Martinez-Garzon, P., Bohnhoff, M., Min, K.-B., Fokker, P., Westaway, R., Bethmann, F., Meier, P., Yoon, K.S., Choi, J.W., Lee, T.J., Kim, K.Y., 2019. First field application of cyclic soft stimulation at the Pohang Enhanced Geothermal System site in Korea. Geophysical Journal International 217(2), 926-949.
- Lee, K.-K., Ge, S., Ellsworth, W.L., Giardini, D., Townend, J., Shimamoto, T., 2019. Summary report of the Korean Government Commission on relations between the 2017 Pohang earthquake and EGS project, in: Lee, K.-K. (Ed.) Geological Society of Korea. The Geological Society of Korea, p. 205.
- Zang, A., Yoon, J.S., Stephansson, O., Heidbach, O., 2013. Fatigue hydraulic fracturing by cyclic reservoir treatment enhances permeability and reduces induced seismicity. Geophysical Journal International 195(2), 1282-1287.

HELMHOLTZ